AUTOMATED PARALLEL CFD ANALYSIS OF INTERNALLY COOLED TURBINE BLADES

D.I. Papadimitriou, K.C. Giannakoglou

Lab. of Thermal Turbomachines,
National Technical University of Athens,
P.O. Box 64069, 15710, Athens, Greece,
e-mail: kgianna@central.ntua.gr

E. Carelas, I. Triantafyllos, G.O. Freskos

Hellenic Aerospace Industry.
Engines Engineering Dept.
PO Box 23, GR-32009 Schimatari, Greece,
e-mail: gfreskos@haicorp.com

Keywords: Turbine,Internal Cooling,Heat transfer,Navier–Stokes,Thermal Fatigue

Abstract. *A computational procedure for the analysis of heat and fluid flow problems around and over internally cooled turbine blades is presented. Integrated to an automated software, this analysis tool is capable of computing the temperature field developed over blades without or with protecting coatings; further insight can be gained by linking the present software with a commercial fatigue analysis software.*

The analysis of the heat and flow problem in cooled turbine blades requires the interacting analysis of (a) the heat and flow fields of the fluid flowing between the turbine blades, typically modeled by the 3D Navier–Stokes equations, (b) the temperature field developed over the blade material, modeled by the Laplace equation and (c) the coolant flow within the cooling passage, for which a 1D convection model seems to be adequate.

The three subproblems' tools interact strongly with each other in the framework of an iterative algorithm. The repetitive calls to 3D field solvers is associated with high computive cost. A considerable reduction of the total ellapsed computing time is achieved through parallelization on a cluster of interconnected processors and multigrid for unstructured grids.

The analysis of the second–stage vane of the high–pressure turbine of a two–spool, low by–pass ratio turbofan engine is presented.

1 INTRODUCTION

The design of internally cooled turbine blades aims to the highest possible overall efficiency which may be interpreted as low exhaust–gas emissions combined with low operating cost. Among others, the achievement of these targets can be obtained, by increasing the operating temperature, i.e. the inlet temperature to the first turbine stage. On the other hand, high operating temperatures lead to thermal fatigue, one of the most important reasons for blade failure. The use of better materials, internal/external blade cooling and/or Thermal Barrier Coatings (TBC) are the main techniques to overcome this problem, [1],[2],[3].

The complete analysis of internally cooled blades requires the combined use of complementary computational tools for each one of the constituent subproblems in the context of an iterative algorithm, in which the converged solution is reached through the regular communication between them. Dealing with an internally cooled turbine blade cascade with fixed geometry, fixed blade material properties, known inlet–outlet flow conditions for the working fluid and known inlet temperature and mass flow rate for the coolant, the ultimate output of such a computation is the temperature field over the blade material. A 3D Navier–Stokes solver with turbulence model for the working fluid, a 3D Laplace equation solver for the

heat transfer modeling over the blade material and an 1D mass and energy conservation model for the coolant flow determine the three major tools required. Used sequentially, each of them provides boundary conditions for the next tool up to the final convergence; the total number of cycles needed determines the overall CPU cost. Needless to say that the two field solvers (i.e. the 3D Navier–Stokes and the 3D Laplace equation solvers) are the most time consuming parts of the computation. Though the Navier–Stokes solver has incomparably higher CPU cost than the Laplace equation solver, it should be stressed out that the latter needs to be solved much more times than the former, so the overall costs of the two tools are practically comparable. To reduce their costs, parallelization and multigrid are used. The existence of TBC on the blade surface is taken into account by means of effective thermal conductivities, as it will be explained below.

The second stage vane of the high–pressure turbine of a two–spool, low by–pass ratio military turbofan engine is analyzed using the aforementioned tools. At the postprocessing level, a preliminary stress and fatigue analysis is also presented.

2 COMPUTATIONAL TOOLS – OVERALL ITERATIVE ALGORITHM

In this section, the computational tools required as well as the overall iterative algorithm are presented. Emphasis is put to the proper interfacing between the various tools, through repetitively updated boundary conditions

2.1 3D grid generation and partitioning

The 3D unstructured grids used for the solution of the Navier-Stokes equations and the Laplace equation consist of tetrahedral elements, generated with coincident nodes over their common surface (external blade surface). The grid around the blade was generated through splitting a 3D structured grid into tetrahedral elements. There is no particular reason for proceeding this way and a pure 3D unstructured grid could otherwise be generated just like the 3D grid used inside the blade material. The latter was generated by importing the surface unstructured grid around the blade (as resulted from the conforming triangulation of the surface grid) into $MSc\ Patran$. No grid is used in the cooling passage. The 3D unstructured grids are decomposed into non–overlapping subdomains, each of which is associated with a different processor of the multi–processor platform available at NTUA. This partitioning is carried out by means of an in–house software based on genetic algorithms [4]. The objective of the partitioner is to divide the grid into a number of subdomains with equal number of tetrahedra each and minimum interface that ensures minimum inter–processor communication during the numerical solution of the partial differential equations.

2.2 The Navier–Stokes solver

The Favre averaged Navier–Stokes equations, coupled with a two–equation $k-\epsilon$ turbulence model, [5], and the wall function technique are solved. The governing equations are discretized and solved using a time–marching, vertex–centered, finite–volume scheme. Convective fluxes are computed in an edge–wise manner by means of the Roe's approximate Riemann solver [6]. Second–order spatial accuracy is achieved through variable extrapolation [7]. The computation of the diffusive fluxes is based on the assumption of linearly distributed flow variables in each element.

The wall function model for the thermal fluxes across the blade surface is based on the Jayatillaka correlation

$$T^+ = \rho c_p u_\tau \frac{(T-T_{wall})}{q_{wall}} = \begin{cases} Pr_t[u^+ + J(\frac{Pr}{\mathrm{Pr}_t})] & , \text{ if } y^+ < 11.6 \\ Pr\ y^+ & , \text{ if } y^+ > 11.6 \end{cases} \quad (1)$$

where

$$y^+ = \frac{\rho {c_\mu}^{1/4} k^{1/2} \delta}{\mu} Re_o \ , \ u^+ = \frac{V_t {c_\mu}^{1/4} k^{1/2}}{\tau_w} \ , \ u_\tau = (\frac{\tau_w}{\rho})^{1/2} \quad (2)$$

$$\tau_w = \begin{cases} \frac{\mu}{Re}\frac{V_t}{\delta} & , \text{ if } y^+ < 11.6 \\ \rho {c_\mu}^{1/4} k^{1/2} \frac{V_t}{\frac{1}{\kappa} ln(y^+) + B} & , \text{ if } y^+ \geq 11.6 \end{cases} \quad (3)$$

where T is the temperature of the last node adjacent to the wall, T_{wall} is the wall temperature and q_{wall} is the heat flux from the gas to the blade.

The J correlation is given by, [8]

$$J(\frac{Pr}{Pr_t}) = 9.24[(\frac{Pr}{Pr_t})^{3/4} - 1][1 + 0.28exp(-0.007\frac{Pr}{Pr_t})] \tag{4}$$

where Pr and Pr_t are equal to 0.72 and 1 respectively.

2.3 Heat transfer analysis over the blade

The thermal fluxes computed by the Navier–Stokes wall functions are used as boundary condition for the solution of the Laplace equation

$$\nabla \cdot (k\nabla T) = \frac{\partial}{\partial x}(k\frac{\partial T}{\partial x}) + \frac{\partial}{\partial y}(k\frac{\partial T}{\partial y}) + \frac{\partial}{\partial z}(k\frac{\partial T}{\partial z}) = 0 \tag{5}$$

in the interior of the blade. This equation is solved on an unstructured grid, using finite–volumes and an edge–based discretization.

Over the blade, the Laplace equation is solved by imposing Neumann (prescribed $\frac{\partial T}{\partial n}$) along the outer and Dirichlet boundary conditions (prescribed T) along the inner surface. Adiabatic conditions are imposed along the hub and shroud edges of the blade, in the absence of any other data.

In the presence of TBC, the solution algorithm remains unaffected and the thermal conductivity coefficient k used in equation 5 is locally modified. However, practically, the TBC thickness is too small compared to the average blade thickness so none of the internal nodes are expected to belong to the coating. In addition, due to the edge based discretization, a thermal conductivity value for each segment is needed. Consequently, segments that belong partially or entirely (boundary segments) to the coating region are given an effective thermal conductivity k_{eff} according to the equation

$$\frac{\delta}{k_{eff}} = \frac{\delta_1}{k_1} + \frac{\delta_2}{k_2} \tag{6}$$

where $\delta = \delta_1 + \delta_2$ is the length of the segment, δ_1,k_1 are the length and the thermal conductivity of its part belonging to TBC and δ_2,k_2 are the same quantities for the rest of the segment.

By doing so, the temperature distribution on the external boundary nodes is that of the outer surface of the coating. Should the temperature on the inner coating surface be required, this can be calculated through post–processing.

2.4 The 1D coolant flow model

The cooling air flows through the blade passage from shroud to hub and the 1D model built for it is based on:

(a) The energy conservation equation written between two radial positions (index i)

$$Q_n = mc_p(T_{c(i)} - T_{c(i-1)}) \tag{7}$$

where Q_n is the heat transfer to the coolant occuring between the two radial positions $i-1$ and i , $T_{c(i-1)}, T_{c(i)}$ the coolant temperatures at these positions, m the coolant mass flow rate and c_p its thermal capacity under constant pressure.

(b) The heat transfer convection equation between the wall and the coolant

$$Q_i = hA_i(T_{w(i)} - T_{c(i)}) \tag{8}$$

where Q_i is the heat transfer to the coolant across the area A_i associated with the radial position i, $T_{w(i)}, T_{c(i)}$ the internal wall and the coolant temperature and h the heat conduction coefficient.

2.5 Parallel processing - Multigrid

The Navier–Stokes and Laplace equations are parallelized using Parallel Virtual Machine, PVM [9] protocol and solved in a cluster of 16 interconnected processors. The solution of the above equations is supported by a multigrid technique [10] which yields about ten times faster convergence for the Laplace equation and

four times for the Navier–Stokes.

2.6 The overall iterative algorithm

The iterative algorithm is illustrated in fig. 1. Considering an initial temperature distribution along the outer vane surface, the Navier-Stokes equations are first solved. An outcome of this solution is the heat flux distribution along the outer surface of the blade, which is then used as boundary conditions for the Laplace equation. The boundary condition for the inner surface of the blade comes from an initial guess of the temperature distribution along it.

The Laplace equation is solved over the blade material and its 3D temperature distribution is computed. The heat flux on the inner blade surface together with the inlet coolant temperature and the coolant mass flow rate are used for the solution of the 1D coolant flow equations. The coolant and the inner blade surface temperature radial distribution are computed; the latter forms the new boundary conditions for the Laplace equation which is solved again, up to the final convergence of the *inner loop*.

Upon completion of the inner loop, the temperature distribution of the outer blade surface is updated, the flow equation are solved anew with the new boundary conditions and this will be referred to as the *outer loop* or *cycle*.

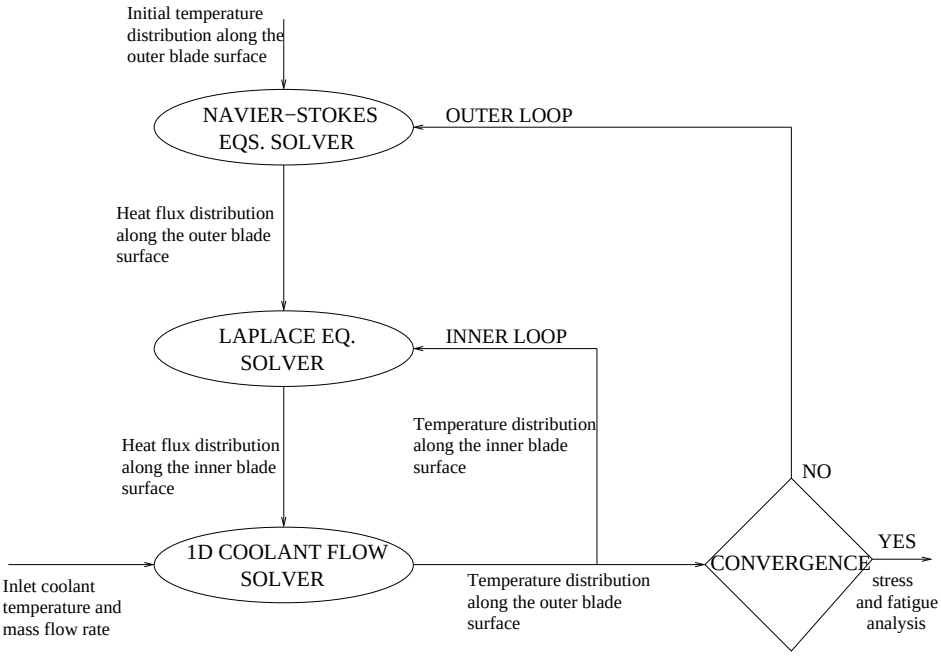

Figure 1: Overall iterative algorithm.

2.7 Stress and fatigue analysis

After the convergence of the algorithm, the temperature distribution at the interior of the vane is known and therefore a thermal stress analysis can be undertaken to compute the stresses developed within the vane. In order to perform this analysis, the model data is then converted to neutral file format and imported to PATRAN for pre-processing and set up of a thermal analysis. The solution of the Finite Element Analysis problem produces the stress distribution in the vane due to the temperature gradient and the geometrical constraints that are imposed to it.

The stresses found are then varied using a simple load history that represents the thermal cycling of the component during engine operation, setting up a crack initiation problem for the PATRAN/FATIGUE module, in order to evaluate its life until a crack appears.

The stress distribution according to the computed temperature distribution is varied, in order to simulate a representative change of throttle settings (or mission profile for the engine). In the present case the loading was varied from zero to the maximum found by the stress analysis (loading history).

3 METHOD APPLICATION–RESULTS

The proposed algorithm has been used for the analysis of the heat and fluid flow in the internally cooled turbine vane of a turbofan engine for which data are available in the Hellenic Aerospace Industry. In fig. 2 the unstructured grids constructed around and inside the blade are shown, with the different colours on the left denoting the 16 grid partitions. The number of tetrahedra for each grid is 475200 and 145447, respectively.

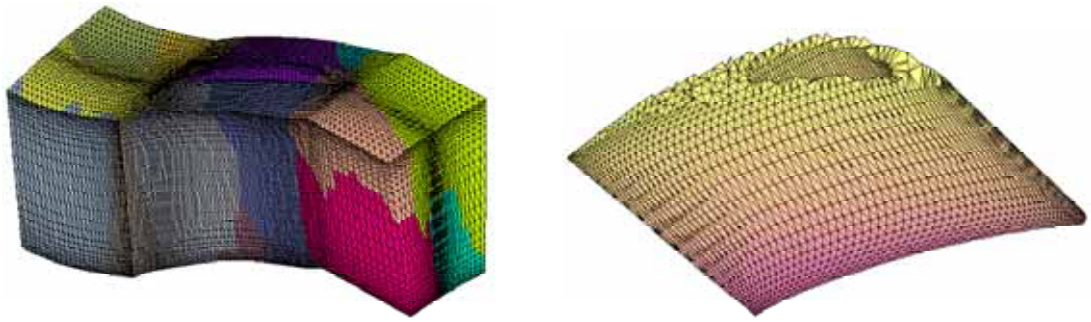

Figure 2: Left: Unstructured grid for the discretization of the inner–vane passage, partitioned into 16 subdomains for parallel processing. Right: Unstructured grid inside the vane.

The inlet total temperature, inlet total pressure and outlet static pressure are $1153K$, $7.6bar$ and $5.3bar$ respectively and the inlet flow is axial. These flow conditions correspond to an inlet Mach number around 0.35 and an exit Mach number around 0.65. The computed iso–Mach number around the vane is shown in fig. 3 which indicates a slightly transonic flow pocket over the first part of the blade suction side, just after the leading edge.

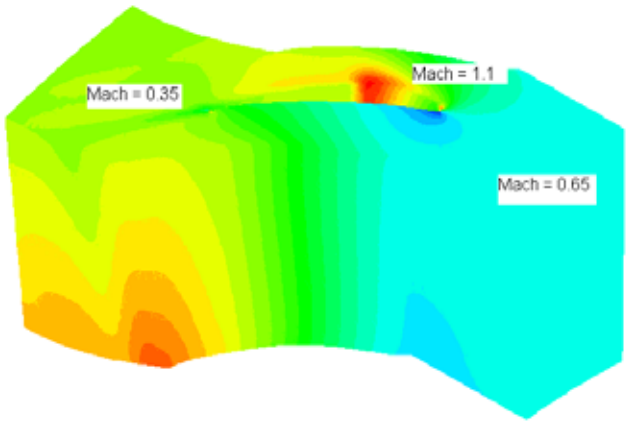

Figure 3: Mach number distribution in the grid around the vane.

The temperature distribution computed over the blade material is shown in fig. 4. The higher temperatures (900-950K) are met close to the trailing edge, i.e. at a region which is far away from the cooling passage and is characterized by high–valued heat transfer coefficients. Around and close to the cooling passage, the temperature value is lower and it is increased again (800-850K) close to the leading edge; though in this area the heat transfer coefficient reaches its highest value, the temperature is kept lower than that of the trailing edge due to the coolant effect. Near the cooling passage, the temperature increases along its flow direction from shroud to hub; we recall that the coolant flows from shroud to hub.

For the considered multi–physics application which is based on repetitive calls to various solvers, it is important to have a clear estimate of the computational cost. So, fig. 5 (left) shows the evolution of the coolant temperature at three indicative radial positions, in terms of the number of cycles. Though this figure shows results for 15 cycles, it can be seen that the results are considered to be converged after approximately the 8th cycle. Fig. 5 (right) illustrates the convergence characteristics of the algorithm

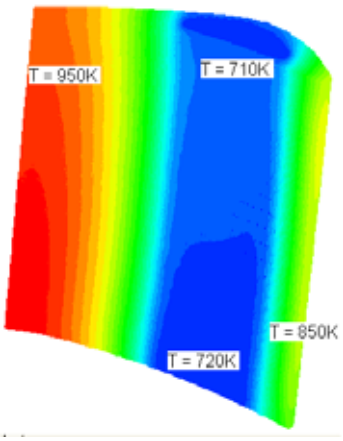

Figure 4: Temperature distribution inside the blade. Minimum temperature: 700K, maximum temperature: 1100K. The coolant flows downwards.

from a different point of view. The radial distribution of the coolant temperature at each cycle (the one computed upon convergence of the inner loop) is plotted. After the first few cycles, all curves become clustered around the converged one.

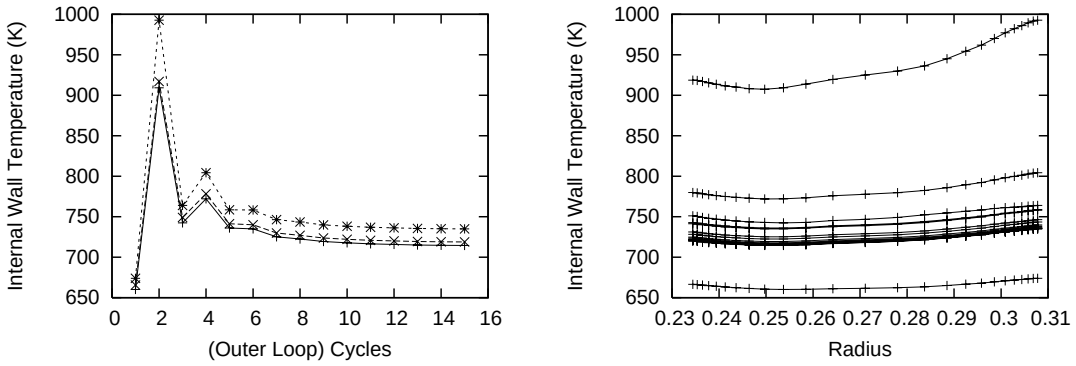

Figure 5: Coolant temperature at three radial positions along the blade (left) and radial distributions of the peripherally averaged internal wall temperature (right). Convergence during the first 15 outer loop cycles.

The next study is concerned with the presence of TBC and its effect on blade cooling. The TBC thermal conductivity is $22W/mK$ (i.e. two orders of magnitude less than that of the blade material) and its thickness is $6\mu m$. Using TBC, the coolant temperature in the passage is increased less than

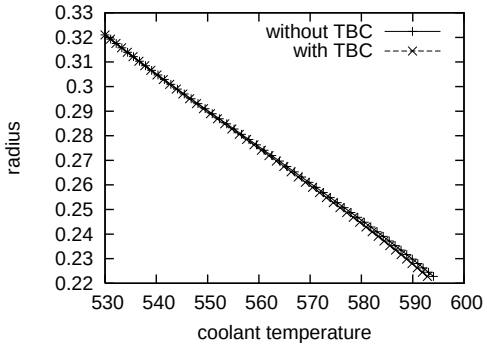

Figure 6: Radial distribution of the coolant temperature with and without TBC.

without TBC, as shown in fig. 6. The temperature at the external blade surface is increased, whereas the temperature below TBC is lower, leading thus to milder thermal loads.

The CPU cost for 15 (outer loops) cycles of the total algorithm is almost 48 hours. Half of the cost is associated with the Navier–Stokes solver (15 calls) and the other half is consumed by the inner loop (15 calls) which consists of 10 consequent calls to the Laplace and the coolant flow solvers.

The Von–Mises Stress tensor distribution over the blade computed using the Msc Patran–Nastran Software is shown in fig. 7 (left). Higher values of stress are met on the hub and the shroud of the vane, where no displacement is allowed and the temperature values are quite high. In fig. 7 (right), the number of cycles needed for blade failure is shown, after the fatigue analysis.

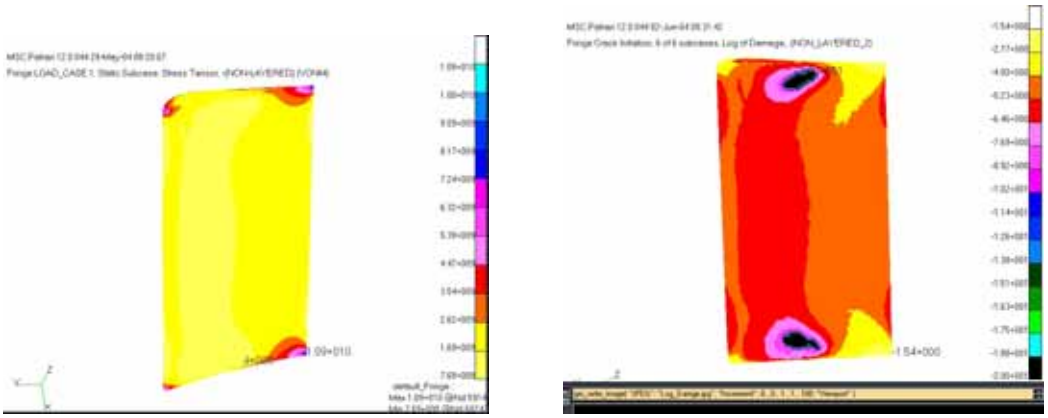

Figure 7: Left: Distribution of stresses over the vane. Right: Total cycles needed for blade failure.

4 CONCLUSIONS

A 3D Navier–Stokes solver, a 3D heat transfer model and a 1D coolant flow analysis tool have been implemented in the context of an iterative algorithm for the analysis of the heat and fluid flow problems in turbine blades with internal cooling. The proposed algorithm involves an outer and an inner loop for handling the three constituents of the problem at hand, in the most efficient way. The inner loop is responsible for the simultaneous satisfaction of the equations governing the heat transfer over the blade and the coolant flow. The outer loop is responsible for the communication of the above subsystems with the flow developed around the blade. It was shown that about 8 outer loops are enough to get a converged solution. The overall computing cost depends on the two field solvers and can be kept at reasonable levels for industrial use through multiprocessing and multigrid. With a 3D flow grid of about 475000 tetrahedra and an internal blade grid of about 145000 tetrahedra the elapsed time was about 2 days on a cluster of 8 Pentium (2400MHz) processors.

The developed tool can be used in the context of design optimization of internally cooled turbine vanes (optimal location, size and shape of the cooling passage) in combination with a 'black box' optimization method, such as evolutionary algorithms; only a few similar works can be found in the literature ([11],[12]), not necessarily using the same analysis tools.

5 ACKNOWLEDGMENT

This work was funded by the Hellenic Aerospace Industry within the framework of a PAVET project (funded by the Hellenic General Secreteriat of Research an Technology). The first author was supported by a grant from the Beneficial Foundation Alexandros S. Onasis.

References

[1] C. Liess. Introduction to cooling of gas turbine blades. Von-Karman Institute Lecture Series, April 1969.

[2] T. Arts. Aero–thermal performance of internal cooling systems in turbomachines. Von-Karman Institute Lecture Series 2000-03.

[3] C. Riegler. Correlations to include heat transfer in gas turbine performance calculations. Aerospace Science and Technology, 1999.

[4] A.P. Giotis and K.C. Giannakoglou. An unstructured grid partitioning method based on genetic algorithms. *Advances in Engineering Software*, 1998.

[5] B.E. Launder and Spalding D.B. The numerical computation of turbulent flows. *Comp. Meth. in Appl. Mech. and Eng.*, 103:456–460, 1974.

[6] P. Roe. Approximate Riemann solvers, parameter vectors and difference schemes. *J. of Comp. Phys.*, 43:357–372, 1981.

[7] B. van Leer. Flux vector splitting for the Euler equations. Lecture Notes in Physics, Vol. 170, pp. 405-512, 1982.

[8] C. L. Jayatillaka. The influence of Prandtl number and surface roughness on the resistance of the laminar sublayer to momentum and heat transfer. *Progress in Heat and Mass Transfer*, 1:193–321, 1969.

[9] A. Geist, A. Beguelin, J. Dongarra, W. Jiang, R. Manchek, and V Sunderam. *PVM: Parallel Virtual Machine. A user's guide and tutorial for networked Parallel Computing.* The MIT Press, 1994.

[10] N.K. Lambropoulos, D.G. Koubogiannis, and K.C. Giannakoglou. Acceleration of a Navier–Stokes equation solver for unstructured grids using agglomeration multigrid and parallel processing. *Computer Methods in Applied Mechanics and Engineering*, 193:781–803, 2003.

[11] T.J. Martin and G.S. Dulikravich. Aero-thermal analysis and optimization of internally cooled turbine airfoils. Proc. of XIII International Symposium on Airbreathing Engines-ISABE, 1997.

[12] T.J. Martin and G. S. Dulikravich. Aero-thermal analysis and optimization of internally cooled turbine airfoils. ISABE 97-7165, 1997.